CONTROLLED RELEASE OF CHLORHEXIDINE FROM A MESOPOROUS SILICA-CONTAINING MACROPOROUS TITANIUM DENTAL IMPLANT PREVENTS MICROBIAL BIOFILM FORMATION

K. De Cremer[1,2,§], A. Braem[3,§], E. Gerits[1], K. De Brucker[1], K. Vandamme[4], J.A. Martens[5], J. Michiels[1], J. Vleugels[3], B.P.A. Cammue[1,2] and K. Thevissen[1,*]

[1] Centre of Microbial and Plant Genetics, KU Leuven, Leuven, Belgium
[2] Department of Plant Systems Biology, VIB, Ghent, Belgium
[3] Department of Materials Engineering, KU Leuven, Leuven, Belgium
[4] Biomaterials-BIOMAT, Department of Oral Health Sciences and Prosthetic Dentistry, KU Leuven and University Hospitals Leuven, Leuven, Belgium
[5] Centre of Surface Chemistry and Catalysis, KU Leuven, Leuven, Belgium

[§] These authors contributed equally

Abstract

Roughened surfaces are increasingly being used for dental implant applications as the enlarged contact area improves bone cell anchorage, thereby facilitating osseointegration. However, the additional surface area also entails a higher risk for the development of biofilm associated infections, an etiologic factor for many dental ailments, including peri-implantitis. To overcome this problem, we designed a dental implant composed of a porous titanium-silica (Ti/SiO_2) composite material and containing an internal reservoir that can be loaded with antimicrobial compounds. The composite material consists of a sol-gel derived mesoporous SiO_2 diffusion barrier integrated in a macroporous Ti load-bearing structure obtained by powder metallurgical processing. The antimicrobial compounds can diffuse through the porous implant walls, thereby reducing microbial biofilm formation on the implant surface. A continuous release of µM concentrations of chlorhexidine through the Ti/SiO_2 composite material was measured, without initial burst effect, over at least 10 days and using a 5 mM chlorhexidine solution in the implant reservoir. Metabolic staining, CFU counting and visualisation by scanning electron microscopy confirmed that *Streptococcus mutans* biofilm formation on the implant surface was almost completely prevented due to chlorhexidine release (preventive setup). Moreover, we demonstrated efficacy of released chlorhexidine against mature *Streptococcus mutans* biofilms (curative setup). In conclusion, we provide a proof of concept of the sustained release of chlorhexidine, one of the most widely used oral antiseptics, through the Ti/SiO_2 material thereby preventing and eradicating biofilm formation on the surface of the dental implant. In principle, our flexible design allows for the use of any bioactive compound, as discussed.

Keywords: Porous titanium, mesoporous silica, controlled release, chlorhexidine, *Streptococcus mutans*, dental implant, *in-situ* drug delivery, peri-implantitis, biofilm.

*Address for correspondence:
Karin Thevissen
Centre of Microbial and Plant Genetics (CMPG) KU Leuven
Kasteelpark Arenberg 20 box 2460
3001 Leuven, Belgium

Telephone number: +32 16329688
Fax number: +32 16321966
Email: karin.thevissen@kuleuven.be

Introduction

The increased use of implanted medical devices in humans (a trend which is likely to continue with aging populations) largely explains the rise in infectious implant complications. Foreign organisms can be introduced into the body during implant installation and the implant surface often forms an ideal substrate for adhesion of microbial cells, the initial phase of biofilm formation (Busscher *et al.*, 2010; Donelli and Vuotto, 2014; Ribeiro *et al.*, 2012). Peri-implant infections can also occur in later phases of implant therapy. In the case of dental implants for example, infections can occur by bacterial contamination (*e.g.* due to poor oral hygiene or soft tissue complications) or be induced by other factors (*e.g.* because of remaining of crown fixation cement). A higher prevalence of peri-implantitis has been identified for patients with presence or history of periodontal disease and for smokers (Marcantonio *et al.*, 2015).

The emergence of dental implants has introduced such artificial surfaces on which oral bacteria can form biofilms within the oral cavity (Belibasakis *et al.*, 2015). These biofilms can then trigger infection and inflammation of the peri-implant tissue (*i.e.* peri-implantitis), leading to chronic infections and progressive peri-implant bone loss in a number of oral surgery patients. Moreover, rough implant surfaces, which were introduced in the dental market in order to improve osseointegration (Bencharit *et al.*, 2014; Taniguchi *et al.*, 2015; Yuan *et al.*, 2014), are thought to facilitate biofilm formation as the total surface area is increased and 'protected' areas are provided (Belibasakis *et al.*, 2015; Braem *et al.*, 2014; Subramani *et al.*, 2009). Still, there is limited and contradictory evidence on the impact

of implant surface characteristics on peri-implantitis. While several studies reported a positive influence of smooth surfaces on peri-implant health (Esposito *et al.*, 2005; Yuan *et al.*, 2014), others failed to find a correlation between the type of implant surface and marginal bone loss (de Freitas *et al.*, 2011; Nicu *et al.*, 2012; do Prado *et al.*, 2013). Nevertheless, oral biofilm formation seems to be a defining factor for the success or the failure of a dental implant (Subramani *et al.*, 2009) and the prevention and/or elimination of biofilms at the implant surface is the key to tackling peri-implant infections.

In the case of established biofilms, surgical intervention is often required, highlighting the need for new strategies to prevent biofilm formation on the implant surface. One strategy is the development of implant substrates that can resist biofilm formation by microbial pathogens. This can be acquired by physical or chemical material treatments and/or introduction of antimicrobial agents on the material surface. Newly developed antimicrobial surfaces can largely be classified as anti-biofouling, resisting or preventing microbial attachment, and/or bactericidal, killing microbial cells upon contact (Hasan *et al.*, 2013). This is usually achieved by applying surface coatings of either intrinsically anti-adhesive materials (passive coatings) or antimicrobial releasing carrier materials (active coatings) or by modifying the implant surface by altering the surface topography or the surface chemistry (Campoccia *et al.*, 2013; Hasan *et al.*, 2013).

However, these innovative approaches can also entail important drawbacks such as the fragility of such anti-infective surfaces with respect to the mechanical load during dental implant function and the limited effectiveness of release coatings due to the short timeframe following implantation during which therapeutic concentrations of antimicrobials are released (Hickok and Shapiro, 2012). With this in mind, a novel disk-shaped implant material was developed combining the high strength of a macroporous Ti structure and the drug-release functionality of mesoporous SiO₂, enabling a continuous diffusion of bioactive compounds from the feed side to the release side (Braem *et al.*, 2015). In the current study, we aim to realise a proof of concept for the application of this Ti/SiO₂ composite material for a novel dental implant design featuring an internal reservoir which can be (re)loaded with antimicrobial compounds. It is hypothesised that diffusion of antimicrobial compounds through the bulk of the implant from the refillable reservoir can establish a stable continuous release without burst effects over a prolonged period of time, effectively preventing biofilm formation during a longer timeframe. Chlorhexidine was selected as antimicrobial agent in this study, as it is one of the most commonly used and best documented antimicrobials in dentistry. It is available in different forms (mouthwash, gel, aerosol, spray and disks) and is considered to be an effective chemical complement to tooth brushing and flossing (Varoni *et al.*, 2012). The antimicrobial effectiveness of the released chlorhexidine was evaluated using the oral bacterial pathogen *Streptococcus mutans* (*S. mutans*).

Materials and Methods

Composite Ti/SiO₂ disk and implant production

Macroporous Ti disks (Ø 12.2 mm, h = 1.3 mm) were prepared by powder metallurgy. Ti (grade S < 8 μm, Rockwood Lithium, Frankfurt, Germany) and TiH₂ starting powders (grade VM, Rockwood Lithium, Frankfurt, Germany) were mixed under argon in a 90:10 molar ratio using a multidirectional mixer (Turbula T2C, WAB, Muttenz, Switzerland) for 24 h. After powder compaction by die pressing at 50 kN, the disks were stepwise dehydrogenated [heating at 5 °C/min to 450 °C (1 h dwell time), at 2 °C/min to 550 °C (1 h dwell time), at 2 °C/min to 650 °C (1 h dwell time)] and sintered at 850 °C for 5 min in a high vacuum furnace (10^{-6} mbar). For the production of high-strength Ti dental implants, the processing route was slightly modified in order to obtain cylinders of sufficient length. The starting powder mixture was inserted in polymer sleeves (Ø 4 mm prepared by hot dipping; Crocell Super SH25, Lambert Products, Waremme, Belgium) and compacted by cold isostatic pressing at 3000 bar. The resulting cylinders were then stepwise dehydrogenated and consolidated as described above. Sintered cylinders were machined to the final shape using a CNC milling device (TM1, HAAS) applying hard-metal cutting tools and drill bits (DIXI polytool, Le Locle, Switzerland) at high speed. After machining, implants were decontaminated by ultrasonic cleaning in ethanol and acetone for 15 min each and rinsing in distilled water. In order to remove metal debris and restore the original highly interconnective pore structure as required for mass transport through the bulk of the material, acid etching was performed in a 1.5 M HF (40 %, Sigma-Aldrich, Saint Louis, MO, USA) and 4.5 M HNO₃ (65 %, Chem-Lab, Zedelgem, Belgium) aqueous solution for 5 s. After neutralisation with boric acid (Fisher Scientific, Illkirch, France) and extensive rinsing in distilled water, the samples were cleaned using a mixture of ethanol and isopropanol and stored until further use. A representative number of implants was analysed by scanning electron microscopy (SEM; Nova NanoSEM 450, FEI, Zaventem, Belgium) using backscattered imaging and associated energy dispersive X-ray spectroscopy (EDX, EDAX, Tilburg, The Netherlands) to check for organic residue in order to confirm that the samples were sufficiently clean.

Integration of the mesoporous SiO₂ diffusion barrier was done by sol-gel synthesis. A mixture (1:1 volume) of a colloidal SiO₂ suspension (Ludox® HS-40, Sigma-Aldrich, Saint Louis, MO, USA) and an aqueous 0.055 M HCl (37 %, Chem-Lab, Zedelgem, Belgium) solution was magnetically stirred for 10 min. Using an in-house designed sample holder, this sol was injected through the disks or through the internal reservoir of the dental implants using a high pressure pump (880-PU, Jasco, Easton, MD, USA) until the sol could be observed on the outside, to ensure the complete sealing of the internal reservoir from the implant surroundings. Samples were aged overnight at 60 °C followed by a heat treatment at 225 °C in air for 6 h (1 °C/min heating rate, RHF 1200, Carbolite Furnaces, Aartselaar, Belgium) in order to decompose surfactant templates (calcination).
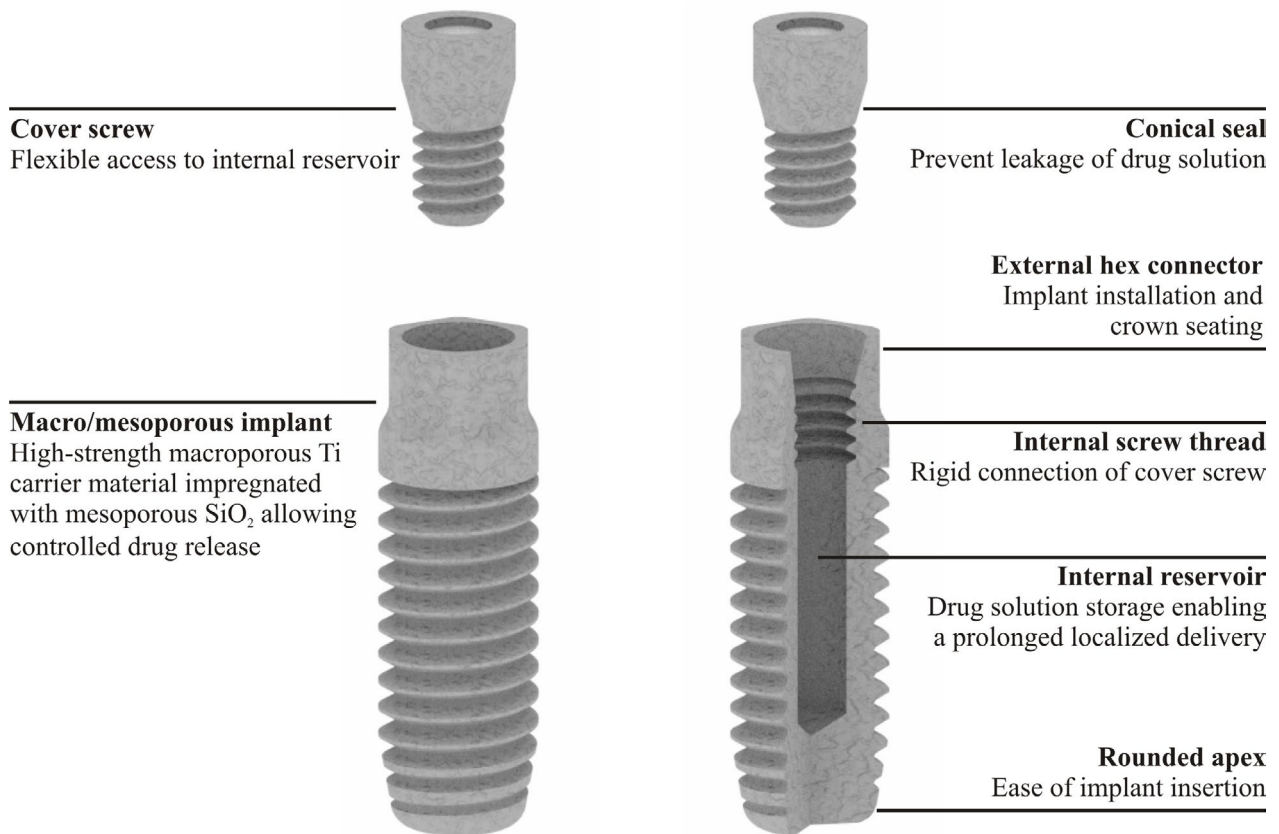
Cover screw
Flexible access to internal reservoir

Conical seal
Prevent leakage of drug solution

External hex connector
Implant installation and
crown seating

Macro/mesoporous implant
High-strength macroporous Ti
carrier material impregnated
with mesoporous SiO$_2$ allowing
controlled drug release

Internal screw thread
Rigid connection of cover screw

Internal reservoir
Drug solution storage enabling
a prolonged localized delivery

Rounded apex
Ease of implant insertion

Fig. 1. Conceptual design for a dental implant enabling a sustained drug release. The one-piece implant/abutment configuration is made out of a mesoporous Ti/SiO$_2$ composite material allowing diffusion of drug molecules from an internal reservoir to the implant surface and surroundings. A cover screw allows easy refilling of the reservoir while the conical seal system prevents leakage of the drug solution to the oral cavity.

Implant design and characterisation

The design of the dental implants is presented in Fig. 1. It was designed to comprise a one piece implant/abutment configuration (Ø 3.5 mm, 8 mm intraosseous length, 3 mm abutment length) for one step surgical installation and immediate restoration without the need of a second surgery for abutment connection. Moreover, an internal reservoir (Ø 1.6 mm, 8 mm of depth) was incorporated in the design for customised drug solution storage allowing prolonged release of antimicrobial compounds through the mesoporous Ti/SiO$_2$ to the implant surface and surroundings. The intraosseous part consists of a M3.5 double lead thread, while the abutment is featured with an external hex connection (hexagonal diameter 3.2 mm). To improve the ease of insertion and to avoid stress concentrations at the implant apex, the apex is slightly rounded (R0.5 mm). A stainless steel cover screw (M2 × 2.25) for flexible refilling of the internal reservoir is equipped with a conical surface mating the 2° countersink in the implant abutment in order to provide a sealing surface that effectively prevents leakage of the drug solution to the oral cavity and *vice versa*. A representative number of polished cross-sections of Ti dental implants, before and after incorporation of the mesoporous SiO$_2$ diffusion barrier, were examined by SEM and EDX, in order to confirm that the SiO$_2$ phase was uniformly distributed into

the Ti macropores in a consistent way. Pore characteristics of the porous Ti dental implants after machining and acid etching were measured by mercury intrusion porosimetry (MIP, AutoPore IV 9500, Micromeretics, Norcross, GA, USA). Characterisation of the mesoporous SiO$_2$ diffusion barrier was done by nitrogen adsorption/desorption at –196 °C (Autosorb 1, Quantachrome, Boynton Beach, FL, USA) using the Brunauer–Emmett–Teller (BET) method and the Density Functional Theory (DFT) method on the adsorption branch of the isotherm to determine the specific surface area and the pore size distribution, respectively. As pre-treatment to remove adsorbed contaminants, the samples were evacuated at 200 °C for 12 h.

Strain and chemicals for release experiments

The *S. mutans* strain Clarke, originally isolated from dental caries (Clarke, 1924), was grown routinely on tryptic soy broth (TSB) agar plates (Becton Dickinson Benelux, Erembodegem, Belgium) at 37 °C for 2 d. Overnight cultures were grown in liquid TSB medium.

Stock solutions of chlorhexidine diacetate salt hydrate (Sigma-Aldrich, Saint Louis, MO, USA) were prepared in Milli-Q water (Merck Millipore, Overijse, Belgium). Artificial gingival crevicular fluid (GCF medium) comprised 40 % human serum and 60 % RPMI medium [RPMI 1640 (pH 7.0) with L-glutamine and without
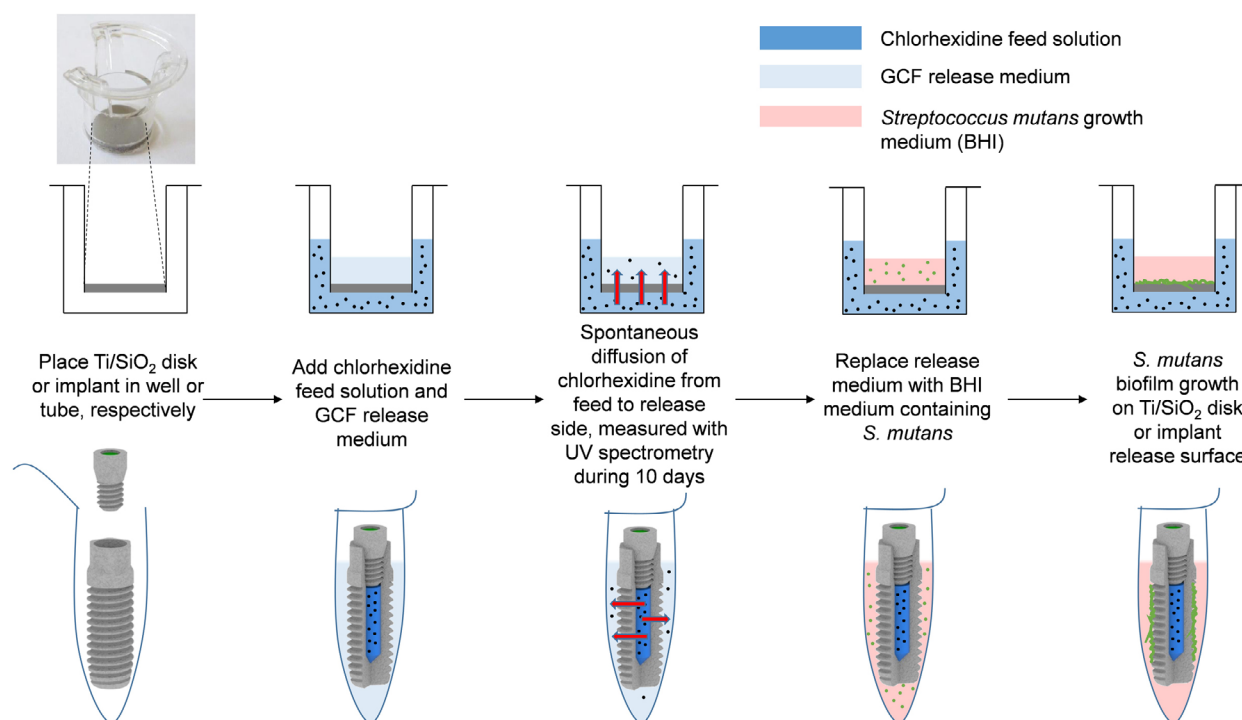
Fig. 2. Schematic representation of the experimental setup of chlorhexidine release experiments and biofilm prevention using Ti/SiO$_2$ disks or implants. The Ti/SiO$_2$ material [grey disk or implant (upper and lower part, respectively)] is placed in its respective container. Chlorhexidine or control solutions (dark blue) and GCF medium (light blue) are administered to feed and release compartments of both settings, respectively. The spontaneous diffusion of chlorhexidine from feed to release side is measured each 2 d using UV spectrophotometry. After 10 d, the GCF release medium is replaced with BHI medium (pink) containing approximately 2×10^6 *S. mutans* cells/mL (green dots) to allow bacterial biofilm formation on the implant material (biofilm prevention). After 72 h, biofilm formation is quantified using metabolic staining and CFU counting or visualised by SEM imaging.

sodium bicarbonate buffered with MOPS (all Sigma-Aldrich, Saint Louis, MO, USA)]. The GCF medium was supplemented with 0.5 μg/mL menadione and 5.0 μg/mL hemin (both Sigma-Aldrich, Saint Louis, MO, USA) as described previously (Dalwai *et al.*, 2006). The BHI (brain-heart infusion) medium (Becton Dickinson Benelux, Erembodegem, Belgium) was supplemented with 3 % sucrose (VWR International, Radnor, PA, USA) for *S. mutans* biofilm growth (Junka *et al.*, 2015). Phosphate buffered saline (PBS) comprised 8 g/L NaCl, 0.2 g/L KCl, 1.44 g/L Na$_2$HPO$_4$ and 0.24 g/L KH$_2$PO$_4$ (pH 7.4; all VWR International, Radnor, PA, USA).

Chlorhexidine Ti/SiO$_2$ disk release experiments
Release experiments using chlorhexidine and the Ti/SiO$_2$ composite material shaped in disks were performed in our previously developed *in vitro* test tool (Braem *et al.*, 2015) with slight alterations which are described here (Fig. 2). Solutions based on Milli-Q water containing different concentrations of chlorhexidine (0, 0.1, 0.25 and 1 mM) (termed feed), were supplied to 12-well plates (1.4 mL/well, 5 wells/condition). Ti/SiO$_2$ disks sealed into polystyrene cups were decontaminated with 100 % ethanol (VWR International, Radnor, PA, USA) and dried under sterile conditions. Sterile disks were placed in the wells

of the 12-well plate, thereby assuring contact between disk and feed solution. On the release side of the Ti/SiO$_2$ disk, we administered 300 μL GCF medium, mimicking natural gingival crevicular fluid (Dalwai *et al.*, 2006), a fluid that is present in the tight anatomical cavity (the so-called periodontal pocket) formed between tooth or implant and periodontal mucosa. Next, the plates were placed in a humidified box to avoid evaporation. The GCF release medium was replaced each 2 d to maintain sink conditions. Chlorhexidine release at 37 °C from the feed side to the release side of the Ti/SiO$_2$ disk was measured in 100 μL of the release medium by UV spectrophotometry [in UV Star microplates (Greiner Bio-One GmbH, Frickenhausen, Germany) with a Synergy Mx multi-mode microplate reader (Biotek, Winooski, VT, USA)]. Absorbance levels were corrected for background absorbance by subtracting the absorbance level of GCF medium recovered from control Ti/SiO$_2$ disks (blank feed solution). A series of solutions containing 6.25-200 μM chlorhexidine in GCF medium were prepared fresh for each day of measurement, in the original GCF medium that was used for the release experiment, to develop a calibration curve. The UV absorbance of 100 μL of each suspension was measured, confirming a linear relationship between absorbance at 255 nm and chlorhexidine concentration over the entire

concentration range that was tested (R^2 = 0.96-0.98). We performed two experiments using two or three independent Ti/SiO$_2$ disks in each experiment (*n* = 5).

To get an indication of the diffusion regime, assuming that the release of chlorhexidine is governed by Fickian diffusion, an estimate of the order of magnitude of the apparent diffusivity was calculated. Fick's first law was applied based on the obtained release data and dimensions of the release system (note that the macropores which contain the SiO$_2$ phase only take up 30 % of the total surface area of the disks) and assuming sink conditions (since the release medium was regularly refreshed) and a path length equal to the thickness of the disks. The value presented is the mean ± SD.

Ti/SiO$_2$ disk biofilm prevention experiment

After 10 d of chlorhexidine release through the Ti/SiO$_2$ disks, the GCF release medium was replaced by 300 µL BHI medium containing approximately 2 × 10^6 *S. mutans* cells/mL (Fig. 2). Biofilms of *S. mutans* were allowed to grow on the release side of the Ti/SiO$_2$ disks for 72 h at 37 °C (renewal of BHI after 48 h), washed with PBS and quantified with the viability dye CellTiter-Blue® (CTB, Promega, Madison, WI, USA) by adding 300 µL CTB diluted 1/10 in PBS to each well. After 2 h of incubation in the dark at 37 °C, fluorescence was measured with a fluorescence spectrometer (Synergy Mx multi-mode microplate reader (Biotek, Winooski, VT, USA) at an excitation wavelength of 535 nm and an emission wavelength of 590 nm. Fluorescence values of the samples were corrected by subtracting the average fluorescence value of CTB of uninoculated disks (blank). Percentage of metabolically active biofilm cells was calculated relative to the control treatment (blank feed solution). We performed two experiments using two or three independent Ti/SiO$_2$ disks in each experiment (*n* = 5). Results were analysed for statistical significance by one-way ANOVA and Bonferroni's correction for multiple testing.

S. mutans biofilms grown on control Ti/SiO$_2$ disks and on Ti/SiO$_2$ disks placed in 1 mM chlorhexidine feed solution were visualised by SEM. Prior to SEM analysis, samples were carefully washed in PBS to remove non-adherent cells and fixed with glutaraldehyde [2.5 % in a cacodylate buffer (0.1 M, pH 7.4); both Sigma-Aldrich, Saint Louis, MO, USA] for 30 min and rinsed 3 times with PBS, followed by dehydration in a series of ethanol washes (30, 50, 70, 90 and 100 % ethanol for 20 min each). Afterwards samples were dried and coated with an Au-Pd layer using a sputtering device (Edwards S150) in order to produce a thin conductive film on the surface. SEM was operated at standard high-vacuum settings at 5 mm working distance and 10 keV accelerating voltage. For samples containing large amounts of organic (biofilm) material at the surface, low-energy imaging using beam deceleration was performed by applying a stage (and sample) bias field, resulting in an effective landing energy of 5 keV.

Ti/SiO$_2$ disk curative biofilm experiment

Biofilms of *S. mutans* were allowed to grow on the release side of the Ti/SiO$_2$ disks by adding 300 µL BHI medium containing approximately 2 × 10^6 *S. mutans* cells/mL.

After incubation for 72 h at 37 °C (renewal of BHI after 48 h), 1.4 mL of chlorhexidine (0.25 mM) or blank control solution was added to the feed compartment. Two days later, biofilms were washed with PBS and quantified with CTB, as described above. Moreover, the amount of colony forming units (CFUs) was determined in biofilms grown on control and chlorhexidine-releasing implants. To this end, the disks were washed with PBS, vortexed vigorously for 1 min, sonicated for 10 min at 45,000 Hz (71.4 W/L) in a water bath sonicator (VWR USC 300-T) and vortexed again. The detached cells were pelleted by centrifugation and washed once more with PBS. A dilution series was established in PBS and 100 µL of each dilution was plated onto TSA plates. After incubation at 37 °C for at least 24 h, the number of CFUs was counted for each condition. The experiment was performed using three independent Ti/SiO$_2$ disks (*n* = 3). Values are presented as mean ± SEM. Results were analysed for statistical significance by unpaired student's *t*-test.

Chlorhexidine Ti/SiO$_2$ implant release experiments and biofilm prevention

Release experiments using chlorhexidine and the Ti/SiO$_2$ composite material shaped in our novel implant design were performed in analogy to the Ti/SiO$_2$ disk experiments (Fig. 2). Ti/SiO$_2$ implants and cover screws were decontaminated with 100 % ethanol and dried under sterile conditions. A solution (termed feed) containing chlorhexidine (5 mM) or blank control solution was administered to the internal reservoir of the implant (10 µL/implant, 3 implants/condition) before closing the reservoir with the cover screw. The implant was placed in a 0.5 mL Eppendorf tube which contained 90 µL of the GCF medium (termed release) and the tube was closed. The GCF release medium was replaced after each 2 d to maintain sink conditions. Chlorhexidine release at 37 °C from the internal reservoir of the implant (feed side) to the release side of the Ti/SiO$_2$ implant (containing the GCF medium) was measured in 70 µL of the release medium by UV spectrophotometry as described above. We performed two experiments using three independent Ti/SiO$_2$ disks in each experiment (*n* = 6).

After 10 d of chlorhexidine release through the Ti/SiO$_2$ implants, the release medium was replaced by 90 µL BHI medium containing approximately 2 × 10^6 *S. mutans* cells/mL (6 implants/condition). Biofilms of *S. mutans* were allowed to grow in the same conditions as described above on the release side of the Ti/SiO$_2$ implants. Quantification of biofilm metabolic activity was performed as described above using 200 µL diluted CTB. Moreover, the amount of CFUs was determined as described above.

To assure that our sonication procedure had no effect on the viability of the *S. mutans* cells, 1 mL of a 10 times diluted overnight *S. mutans* culture was subjected to the sonication procedure. A CFU plating experiment confirmed no effect of sonication on cell viability (*p*-value = 0.859 in unpaired two-tailed students *t*-test ;*n* = 3). Control (without sonication) and sonicated cell cultures both contained approximately 2 × 10^7 CFUs. This cell number was chosen to represent the number of CFUs present in control biofilms formed on the implant surface.

Minimum (biofilm) inhibitory concentration

Minimum inhibitory concentration (MIC) assays were performed in liquid TSB medium. Briefly, overnight cultures of bacteria were diluted in fresh medium to a final concentration of approximately 5×10^5 cells/mL. Next, bacteria were incubated in the presence of a two-fold dilution series of chlorhexidine. After 24 h of growth at 37 °C, bacterial growth was determined by measuring the OD$_{595}$. MIC was interpreted as the lowest antibiotic concentration that completely inhibits bacterial growth.

To assess the anti-biofilm activity of chlorhexidine against *S. mutans*, overnight cultures were diluted 1/200 in BHI medium and two-fold serial dilutions (150 µL) of chlorhexidine in the cell suspensions were prepared in a microtiter plate. After 24 h of biofilm formation at 37 °C, biofilms were washed with PBS and quantified with CTB as described above using 200 µL diluted CTB. The lowest concentration of chlorhexidine required to inhibit biofilm formation was defined as the biofilm inhibitory concentration (BIC).

Cytotoxicity assay

A cytotoxicity test of chlorhexidine was performed on a cell type relevant to bone homeostasis. MG63 osteoblast-like cells, a human osteosarcoma cell line, were obtained from ATCC (American Type Culture Collection CRL-1427, LGC Standards, Molsheim, France). Cells were plated in 24-well plates at 2000 cells/cm² in Minimum Essential Medium Eagle Alpha Modification (αMEM; Sigma-Aldrich, Saint Louis, MO, USA) with 0.292 g/L L-glutamine (G7513, Sigma-Aldrich, Saint Louis, MO, USA) supplemented with 10 % foetal bovine serum (PAA Laboratories GmbH, Pasching, Austria) and 1 % antibiotic-antimycotic (Gibco 15240, Life Technologies SAS, Saint Aubin, France). Cells were maintained overnight at 37 °C in a humidified environment with 5 % CO$_2$. The media were changed every 48 h.

At day 2 post seeding, cells were incubated with chlorhexidine by adding the compound to the culture medium. As a control, a suspension of the same cell line under the same conditions, but without chemicals, was cultured. Dilution assays started at the maximum concentration of 10 µM. Chlorhexidine concentrations were freshly prepared at each time point of addition. The proliferation of the MG63 cells in the presence or absence of chlorhexidine was live investigated by means of a resazurin-based reagent (Presto Blue®, Thermo Fischer, Breda, The Netherlands) after 2, 4 and 6 d of compound addition. The Presto Blue solution (PB) (Life Technologies, Ghent, Belgium) was prepared in a proportion of 10 unit volumes of medium and 1 unit of reagent. The medium in each well was removed and replaced by 0.5 mL of PB. After 2 h incubation, 2 aliquots of 200 µL were taken from each well and transferred to a 96-well plate. The PB solution was completely removed from each well and replaced by 1 mL of culture medium containing the appropriate chlorhexidine concentration. The fluorescent signal was measured with an automated microplate fluorimeter (SerColab Systems, Merksem, Belgium). The blank value was subtracted from the measurement of each group analysed. The experiment was performed twice with duplicate measurements.

Results

Chlorhexidine is released in a controlled way through Ti/SiO$_2$ composite disks and inhibits *S. mutans* biofilm formation

We used our previously developed *in vitro* test tool (Braem *et al.*, 2015) consisting of the Ti/SiO$_2$ composite material shaped into disks (Fig. 2, upper part), as a step-up model to assess the release of the antimicrobial compound chlorhexidine through the mesoporous material and to design the novel implant.

The 10 d release profile of chlorhexidine through the Ti/SiO$_2$ disks, containing different feed concentrations (0.1, 0.25 and 1 mM), is shown in Fig. 3**a**. A steady release of chlorhexidine was apparent from day 3 after the start of the experiment (illustrated by the nearly linear cumulative release profile). Feed solutions of 0.1, 0.25 and 1 mM chlorhexidine released on average 9, 25 and 99 nmol/cm², respectively (corresponding to 33 µM, 89 µM and 359 µM in the release medium). Higher chlorhexidine release was observed for higher feed concentrations at all time points. Moreover, we were able to detect chlorhexidine (> 6.25 µM) in the release medium up to 40 d after the start of the experiment (using 1 mM chlorhexidine feed solution). Based on these release data and assuming that the release of chlorhexidine through the SiO$_2$ phase of the Ti/SiO$_2$ disks is governed by Fickian diffusion, the apparent diffusivity as averaged over the different feed concentrations, was estimated to be $2.0 \pm 0.1 \times 10^{-11}$ m²/s.

Next, we assessed whether the chlorhexidine-releasing material could prevent biofilm formation *in vitro*. Fig. 3**b** shows the metabolic activity of *S. mutans* biofilm cells grown on the release side of Ti/SiO$_2$ disks that were actively releasing chlorhexidine. The metabolic activity of biofilm cells was significantly decreased ($\pm$ 99 % reduction) for all chlorhexidine feed concentrations as compared to blank feed solutions. Bacterial growth on control Ti/SiO$_2$ disks and on chlorhexidine-releasing Ti/SiO$_2$ disks (1 mM feed solution) was visualised by SEM imaging (Fig. 4). Thick *S. mutans* biofilms were formed only on control Ti/SiO$_2$ disks releasing no chlorhexidine. Interconnected mushroom-shaped micro-colonies, consisting of coccus-shaped *S. mutans* cells, were clearly visible within the biofilm, which was spread out over the entire disk surface, covering all pores. On the contrary, the open porosity of the Ti/SiO$_2$ material was still apparent in the chlorhexidine-releasing disks, which contain only few attached *S. mutans* cells (Fig. 4). The lowest released chlorhexidine concentration (33 µM) was able to kill a *S. mutans* culture in a normal vial of BHI medium in less than 24 h. Inhibition of *S. mutans* by chlorhexidine at the released concentrations was expected, since they are well above the MIC (3.2 µM) and BIC (1.6 µM) values. It should be noted that the data obtained in the preventive Ti/SiO$_2$ disk setup were not validated by CFU counting. In this respect, the disk setup should be considered as a preliminary tool which enables us to (relatively quickly) screen more concentrations and compounds (see also Braem *et al.*, 2015). Therefore, only metabolic staining and SEM imaging were used to quantify and visualise biofilm formation in the preventive setup using Ti/SiO$_2$ disks. The following experiments (curative
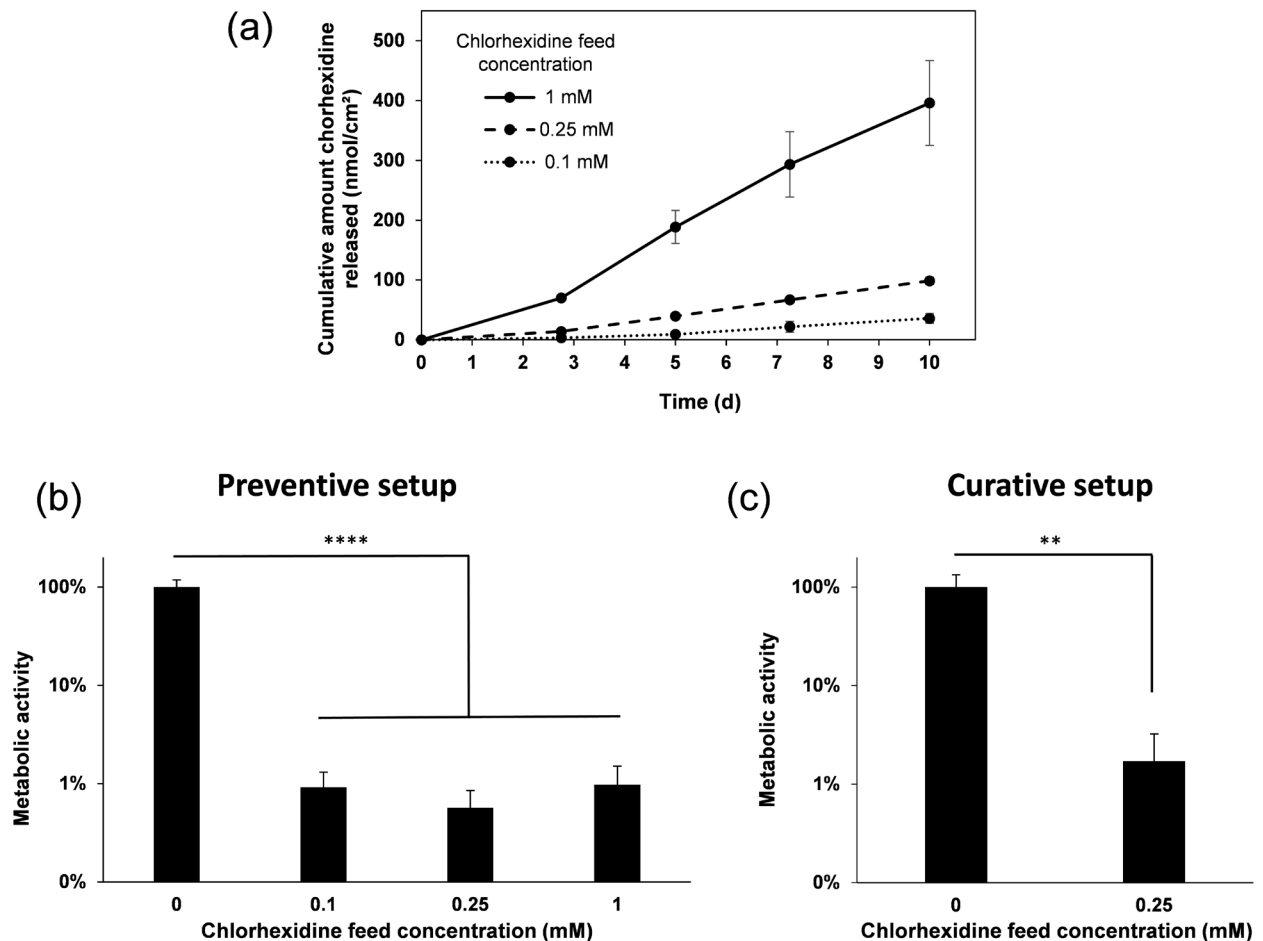
Fig. 3. Release of chlorhexidine through Ti/SiO$_2$ disks and associated effect on *S. mutans* biofilm metabolic activity. (**a**) Cumulative amount of chlorhexidine released through Ti/SiO$_2$ disks in the *in vitro* test tool for different chlorhexidine feed concentrations (measured by UV spectrophotometry at 255 nm). Values are mean ± standard error of two independent experiments containing 2-3 repeats ($n = 5$). (**b**) Prevention of *S. mutans* biofilms on Ti/SiO$_2$ disks. Values are mean metabolic activity ± standard error of two experiments containing 2-3 repeats ($n = 5$), measured by CTB staining. (**c**) Eradication of mature *S. mutans* biofilms on Ti/SiO$_2$ disks. Values are mean metabolic activity ± standard error of two experiments containing 2-3 repeats ($n = 5$), measured by CTB staining. The asterisks indicate a statistically significant difference in metabolic activity (** $p < 0.01$; **** $p < 0.0001$).

---

setup and Ti/SiO$_2$ implant experiments) were additionally validated by CFU counting.

To demonstrate that our material was also suitable for treatment of established infections, *S. mutans* biofilms were allowed to grow on the release side of the Ti/SiO$_2$ disks for 2 d in the absence of chlorhexidine. Administration of 0.25 mM chlorhexidine to the feed compartment after biofilm maturation significantly reduced the metabolic activity (± 98 % reduction) of *S. mutans* biofilm cells after only 2 d of chlorhexidine release (Fig. 3c). CFU counting confirmed that the number of retrieved *S. mutans* biofilm cells was significantly reduced from $1.64 \pm 1.11 \times 10^6$ to $2.68 \pm 1.24 \times 10^4$ ($p = 0.0197$).

Design and characterisation of mesoporous Ti/SiO$_2$ implants with an internal reservoir

Next, we developed dental implants consisting of the Ti/SiO$_2$ composite material (Fig. 1). An internal reservoir was incorporated in the design for customised drug solution

storage allowing prolonged release of antimicrobial compounds through the mesoporous Ti/SiO$_2$ to the implant surface and surroundings.

Fig. 5a shows a backscattered electron image of a cross-sectional detail of the Ti/SiO$_2$ implant near the screw thread crest, indicating an angular macroporous Ti phase with open surface pores. Indeed, mercury intrusion porosimetry of the implant indicated that the open porosity amounted 23.0 % while the average interconnecting pore window size was 1.4 μm after machining and acid etching (Fig. 5c). A representative image of an associated elemental (Ti and Si overlay) mapping can be found in Fig. 5b. This confirmed the uniform distribution of a SiO$_2$ phase throughout the whole Ti pore structure in a consistent way. According to nitrogen adsorption measurements, the final Ti/SiO$_2$ composite dental implant exhibited a pore size distribution ranging from 4 to 10 nm with an average mesopore diameter of 5.8 nm and a specific surface area of 180.7 m²/g SiO$_2$ (Fig. 5d).

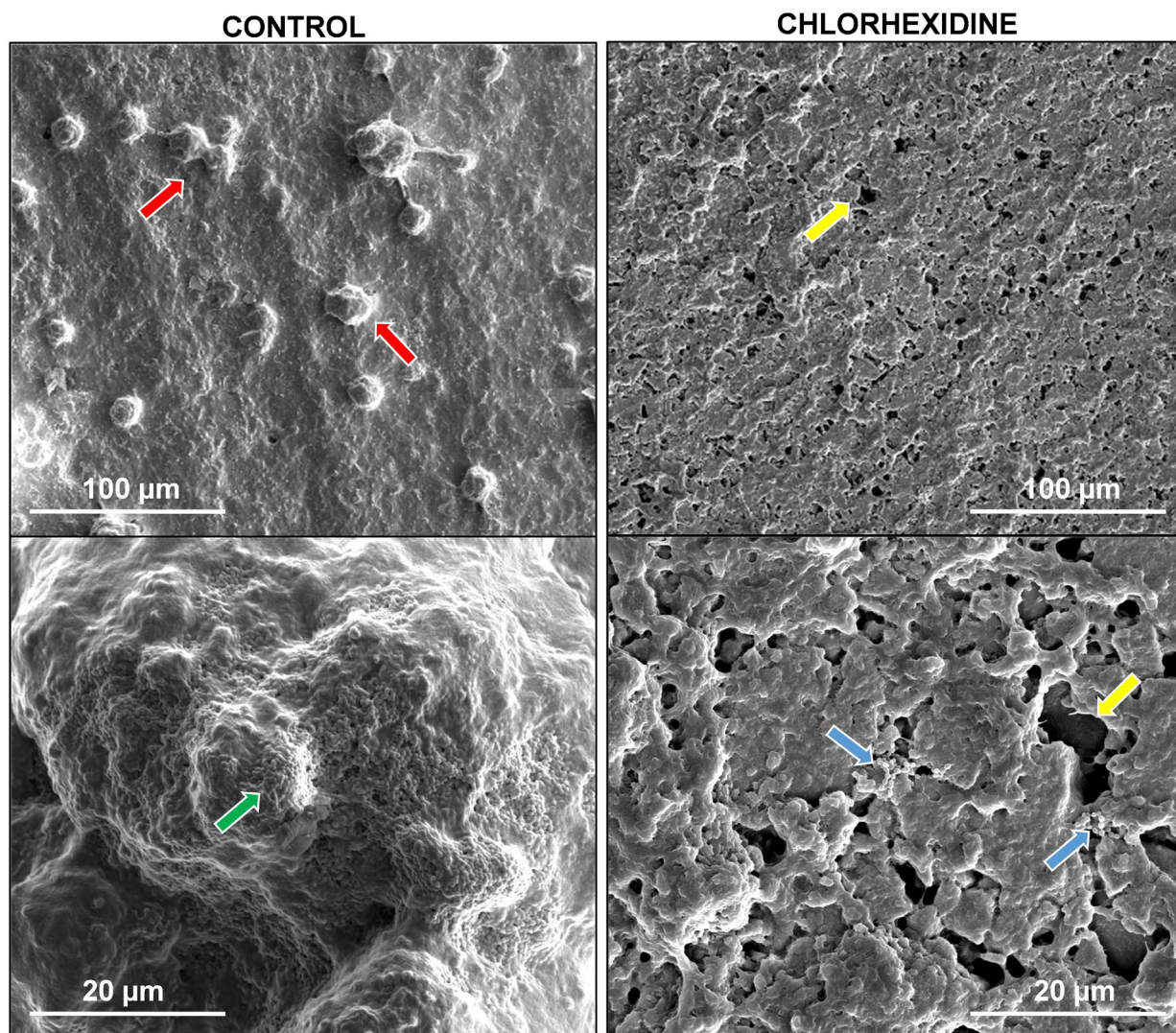**CONTROL**   **CHLORHEXIDINE**

Fig. 4. SEM image of *S. mutans* growth on control (left) and chlorhexidine-releasing (right) Ti/SiO₂ disks. *S. mutans* was allowed to grow on top of Ti/SiO₂ disks following a 10 d release experiment in which control or 1 mM chlorhexidine solution were applied in the feed compartment of the *in vitro* test tool (biofilm prevention). The SEM was operated at standard high-vacuum settings at 5 mm working distance. To avoid beam damage of the biofilm on control disks, low-energy imaging using beam deceleration was performed by applying a stage (and sample) bias field, resulting in an effective landing energy of 5 keV. For chlorhexidine-releasing disks, a 10 keV accelerating voltage was used. The formation of mushroom-shaped micro-colonies (red arrows) consisting of *S. mutans* cells (green arrow) is visible on control disks. On the contrary, the open surface porosity is exposed in chlorhexidine-releasing disks (yellow arrows) which contain only few attached *S. mutans* cells (blue arrows).

Chlorhexidine is released in a controlled way through Ti/SiO₂ composite implants and inhibits *S. mutans* biofilm formation

Using the dental implants characterised above, we confirmed chlorhexidine release through the Ti/SiO₂ composite material from the internal reservoir (5 mM chlorhexidine feed solution, approximately 0.3 %) towards the release side (Fig. 6**a**). Also in this setup, a steady release of chlorhexidine could be measured from day 3 after the start of the experiment (illustrated by the nearly linear cumulative release profile). On average 26 nmol/cm² chlorhexidine were released from the internal reservoir, resulting in an average concentration of 80 µM in the release medium.

The concentration in the release medium depended on the volume of the release medium and on the volume of the feed solution. Since the ratio of feed volume over release volume is 50 times lower in the implant setup, one can expect lower release concentrations in the implant setup using similar feed concentrations. Indeed, using 5 mM chlorhexidine feed solution, the release concentrations were remarkably lower in the implant setup (± 80 µM or 0.005 %) compared to 1 mM feed concentrations in the disk setup (resulting in an average release concentration of 359 µM). The 5 mM feed concentration resulted in release concentrations in the implant set up that were comparable to release concentrations achieved with 0.1-0.25 mM chlorhexidine feed solutions in the disk setup. Significantly
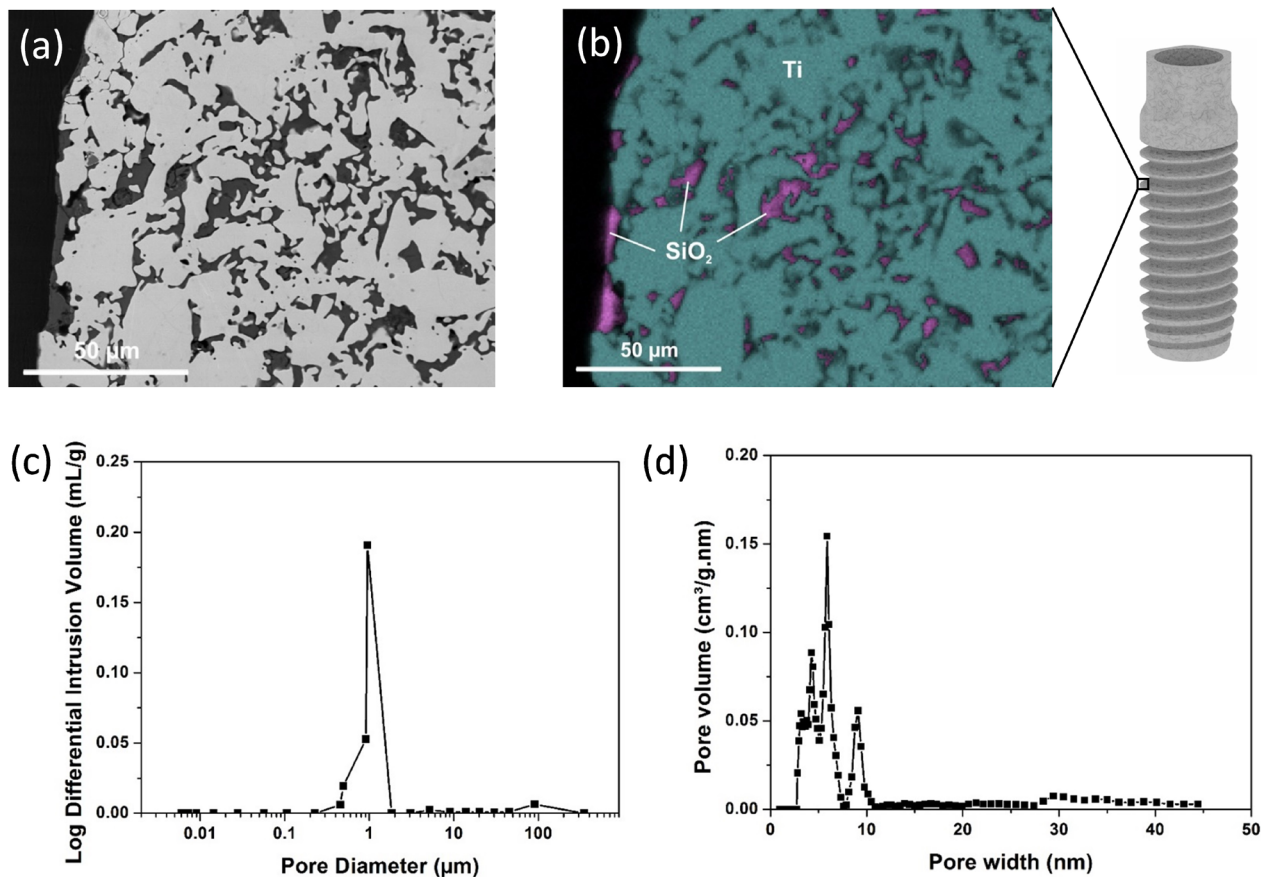
Fig. 5. Combining macro- and mesoporosity in a Ti/SiO$_2$ composite dental implant. A representative cross-sectional detail at the screw thread crest was analysed by SEM using backscattered electron imaging showing (**a**) macroporous Ti (in light grey) and (**b**) associated elemental mapping confirming the presence of a SiO$_2$ phase (magenta) inside the Ti (blue) macropores in a consistent way. (**c**) Prior to SiO$_2$ infiltration, the macroporous Ti implant has a pore window size distribution around 1.4 µm as measured by mercury intrusion porosimetry, while the (**d**) Ti/SiO$_2$ composite dental implant presents a mesoporous structure with an average pore size of 5.8 nm as determined by nitrogen adsorption measurements.
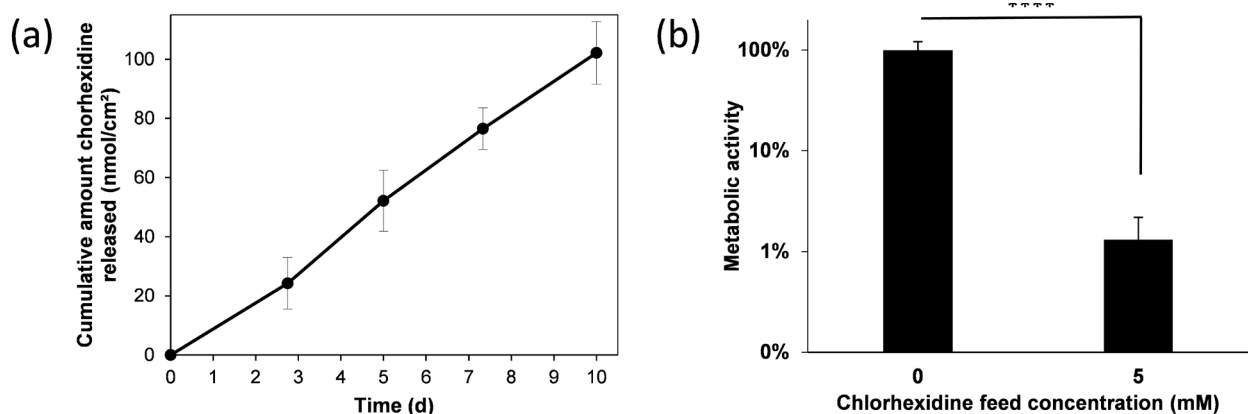

Fig. 6. Release of chlorhexidine through Ti/SiO$_2$ implant and associated effect on *S. mutans* metabolic activity. (**a**) Cumulative amount of chlorhexidine released through Ti/SiO$_2$ implants in the *in vitro* test tool for 5 mM chlorhexidine feed concentration (measured by UV spectrophotometry at 255 nm). Values are mean ± standard error ($n = 3$). (**b**) Metabolic activity of *S. mutans* biofilms grown for 72 h on Ti/SiO$_2$ implants on the implant surface after 10 d of chlorhexidine release. Values are mean ± standard error of two experiments containing 3 repeats ($n = 6$), measured by CTB staining. The asterisks indicate a statistically significant difference in metabolic activity (**** $p < 0.0001$).
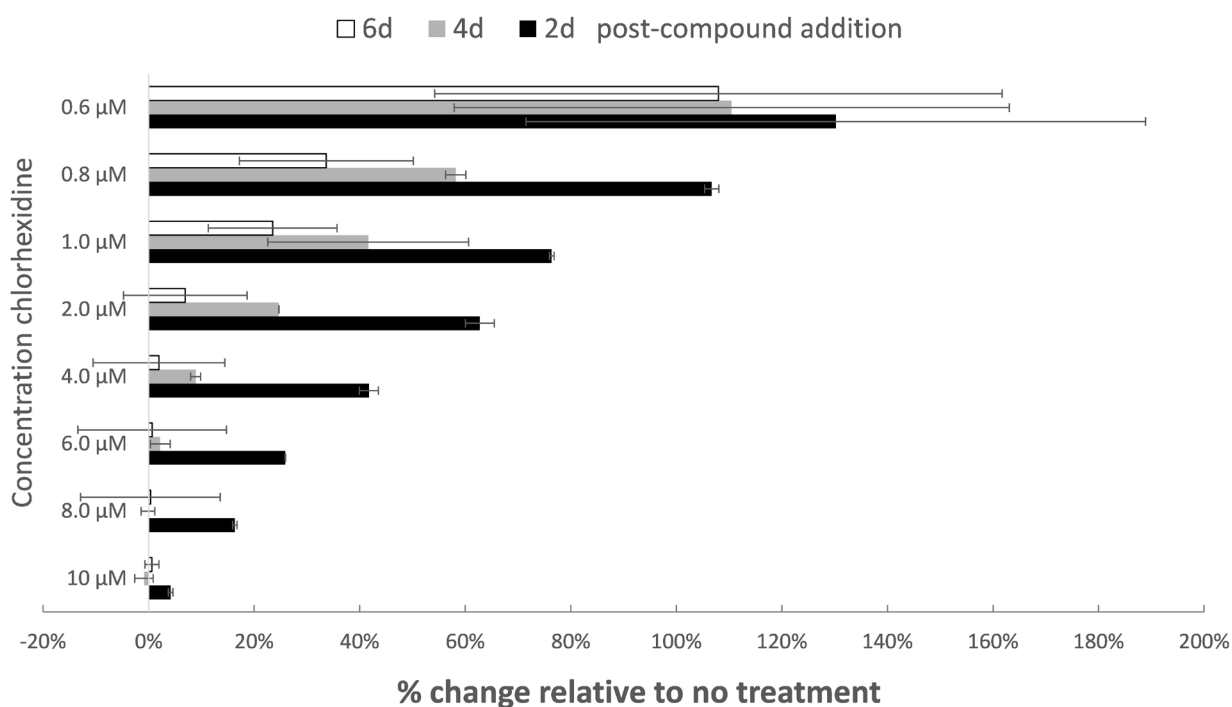
Fig. 7. Effect of chlorhexidine on the viability and growth potential of osteoblast-like cells. MG63 cells were grown in 24-well plates in αMEM. At day 2 post-seeding, the cells were incubated with or without chlorhexidine by adding the compound or mock treatment to the culture medium. MG63 proliferation profiles were evaluated using Presto Blue measurements relative to the no treatment control on the same day, with measurements after 2, 4 and 6 d of compound addition. This figure represents two independent biological experiments consisting of two technical repeats each.

reduced metabolic activity (± 99 % reduction) of *S. mutans* cells growth on chlorhexidine-releasing implants (5 mM feed concentration) was observed compared to *S. mutans* biofilm cells grown on control implants (Fig. 6**b**).

We confirmed these observations by CFU counting of *S. mutans* biofilm cells recuperated from the implants. Biofilms grown on control Ti/SiO$_2$ implants consisted of on average $2.01 \pm 0.55 \times 10^7$ CFU/implant, whereas no CFUs could be retrieved from chlorhexidine-releasing implants. This is, however, an underestimation of the number of recovered CFUs, since *S. mutans* cells could still be detected on the implant surface after sonication (by SEM imaging; data not shown). Nevertheless, it was clear that the residual biofilm was considerably larger on control Ti/SiO$_2$ implants than on chlorhexidine-releasing implants, where only a few remaining cells were observed. This indicated that, although sonication was not sufficient for a complete removal of established biofilms from the implant substrate, CFU counting of recuperated *S. mutans* cells still allowed for a qualitative comparison between the different samples. Moreover, the minimal dilution that was plated on agar was a 10-fold dilution of the suspension in which the biofilm was dissolved, thereby thresholding our quantification to 10 CFUs/biofilm.

Chlorhexidine affects the growth potential of osteoblast-like cells in a dose-dependent manner

Osteoblasts are key players in the processes of establishment and maintenance of implant osseointegration. Therefore, in view of the application of chlorhexidine in preventing/

curing peri-implantitis, we examined the cytotoxic effects of chlorhexidine on MG63 osteoblast-type cells (Fig. 7). At day 2 post-seeding, cells were incubated with chlorhexidine by adding different concentrations of the compounds to the culture medium. To determine the toxicity of chlorhexidine as a function of the various applied concentrations, cell proliferation was determined after 2, 4 and 6 d of incubation and normalised to the no treatment control on the same day. Upon treatment with chlorhexidine up to 1.0 µM, human osteoblast-like cells survived and cell proliferation was permitted, however cytotoxic behaviour (less than 70 % proliferation compared to the no treatment control) of chlorhexidine towards the osteoblasts was apparent for doses above 0.6 µM when cells were treated for more than two days.

Discussion

Implant related infections are a serious complication in prosthetic surgery. Recently, implants with rough surfaces or porous surface coatings are applied for improved osseointegration. However, some studies report that the increased surface roughness renders the implant more susceptible to microbial colonisation and subsequent biofilm formation (Belibasakis *et al.*, 2015; Braem *et al.*, 2014; Subramani *et al.*, 2009). Therefore, the development of implant materials or surfaces that combine both the ability to improve osseointegration and at the same time reduce the infection risk are of interest. The unique implant

design proposed in this study exposes a rough implant surface, while overcoming the reported associated problem of increased bacterial growth by controlled release of chlorhexidine, which is loaded in the internal reservoir, through the Ti/SiO$_2$ composite material.

The capacity of this Ti/SiO$_2$ composite material to transfer the antimicrobial compound chlorhexidine from a feed compartment to a release compartment was assessed in our *in vitro* test tool consisting of Ti/SiO$_2$ disks. It was demonstrated that chlorhexidine diffuses steadily through the mesoporous material over at least 10 d (Fig. 3**a**) and that therapeutically relevant concentrations can be released up to 40 d. The kinetic diameter of chlorhexidine having a molecular size of *ca.* $3.4 \times 0.7 \times 0.6$ nm is within the same range as the pore size (circa 6 nm) of the SiO$_2$ phase of the Ti/SiO$_2$ composite, therefore, the diffusion is governed by a configurational regime as indicated by the apparent diffusivity in the order of 10^{-11} m^2/s (Verraedt *et al.*, 2010).

We assessed the activity of the released chlorhexidine against *S. mutans* biofilms, both in a preventive (to prevent biofilm formation) and curative setup (to eradicate existing biofilms). The choice of the bacterium *S. mutans* in this study should be interpreted as most relevant in the preventive set-up – prevention of the biofilm composition maturation towards anaerobic species by eradicating the preceding aerobic ones. The released chlorhexidine was capable of almost completely preventing *S. mutans* biofilm formation on the release side of the Ti/SiO$_2$ disk (Fig. 3**b** and Fig. 4). In a similar setup, the anti-biofilm effect of toremifene was previously reported against the fungal pathogen *Candida albicans* (Braem *et al.*, 2015), demonstrating the broad flexibility of this system to act against different biofilm-forming pathogens and releasing diverse compounds. Moreover, by adjusting the concentration of the feed solution, the amount of released compound can be fine-tuned (Fig. 3**a**). These features are unique for drug-releasing implant materials, since most implant materials suitable for controlled release of a medical drug are preloaded, releasing only one compound until depletion. Moreover, using these materials, the drug is mainly leached during an initial burst release followed by release at sub-therapeutic concentrations, risking resistance development (Goodman *et al.*, 2013; Lyndon *et al.*, 2014). It should be noted that compounds administered into the periodontal pocket are rapidly washed out *in vivo* (Goodson, 2003). To mimic this situation, we refreshed the release medium every 2 d to maintain sink conditions. GCF flow rates are highly dependent on the disease state with higher values with increasing infection status (from 5 µL/h up to 137 µL/h). Fine-tuning of a continuous flow system for this set-up, thereby discriminating between healthy persons and patients with intermediate or advanced periodontal disease would be most interesting.

Using the Ti/SiO$_2$ disks, we additionally demonstrated activity of released chlorhexidine against mature *S. mutans* biofilms (in a curative setup) (Fig. 3**c**), both using metabolic staining and CFU counting. Consequently, treatment of infections occurring in later stages of implant therapy is possible as well, by adding the desired agent in the reservoir, which is easily accessible. Moreover, this confirms that the observed effect is not merely due to a surface effect but that the chlorhexidine actively kills *S. mutans* biofilm cells.

Controlled release of compounds from the internal cavity through the implant material is a highly novel approach. However, various existing dental implants consist of an internal cavity, not for drug release but to enable dental surgery. Such cavity allows engaging specific surgery tools or screw-retained fixtures, like healing screws, abutments or crowns. The concept of combining hollow tubular metallic support structures including orifices of 0.2 up to 1.0 mm with various drug-releasing carrier materials inside the internal cavity has been previously suggested, among others for percutaneous orthopaedic implants (Clark *et al.*, 2008; Gimeno *et al.*, 2015; Park *et al.*, 2014; Perez *et al.*, 2011; Santos *et al.*, 2014). The novelty of the current design lies in the fact that the mesoporous controlled release (SiO$_2$) matrix is incorporated in the (Ti) implant walls (Fig. 1 and Fig. 5**a**, **b**), rendering the functional implant itself a true drug delivery vehicle. Indeed, current results indicate that the previously described processing route for the Ti/SiO$_2$ composite material (Braem *et al.*, 2015) was successfully transferred to the proposed dental implant design as indicated by the comparable macro- and mesoporous characteristics (Fig. 5**c**, **d**). The controlled release of the molecules applied in the reservoir is governed by their diffusion through the mesoporous SiO$_2$ phase. It is well known that by controlling the pore morphology and/or chemistry of SiO$_2$ materials the diffusion (and hence the release kinetics) of therapeutic molecules can be fine-tuned (Aerts *et al.*, 2010; Bhaskara *et al.*, 2014; Bhattacharyya *et al.*, 2014; Santamaria *et al.,* 2014; Verraedt *et al.*, 2010). We hypothesise that incorporating a SiO$_2$ material with adequate pore characteristics will allow to adapt the system for any specific molecule. Moreover, there is no risk for bacteria to enter the implant, since the mesopores in the Ti/SiO$_2$ are only a few nm in diameter, which is too small for bacteria to enter.

Up to now, the clinical implementation of localised drug delivery around dental implants has been limited to the application of drug eluting coatings on the implant surface or the injection of bioresorbable drug carriers into the peri-implant pocket (Santos *et al.*, 2014). While coatings are fragile and can easily get damaged upon implant insertion (Hickok and Shapiro, 2012), drug carrier materials in the peri-implant gingival pockets are subject to erosion due to masticatory action. With this drug-releasing functional dental implant, a more reliable and more homogeneously distributed antimicrobial release over the entire implant surface area is envisaged and over an extended time period. By applying a 5 mM (approximately 0.3 %) chlorhexidine feed solution in the implant reservoir, we obtained a steady release resulting in on average 80 µM chlorhexidine (approximately 0.005 %) in the release medium over at least 10 d (Fig. 6**a**). However, based on the results from the extended Ti/SiO$_2$ disk experiment, we also can expect a much longer release of active chlorhexidine concentrations from the Ti/SiO$_2$ implant.

Many studies have reported benefits associated with chlorhexidine treatment as preventive therapy against development of peri-implant disease as adjunct to mechanical debridement and basic oral hygiene (Pedrazzi

et al., 2014). Notwithstanding its efficacy, evidence is increasing that chlorhexidine may have deleterious effects on various cell types *in vitro* (Pucher and Daniel, 1992; Cline and Layman, 1992; Mariotti and Rumpf, 1999; Giannelli et al. 2008). Given that osteoblasts represent the main cell type involved in bone tissue regeneration and their function is pivotal for the clinical resolution of periodontal and peri-implant defects (Shibli et al., 2006), the use of chlorhexidine in periodontal and peri-implant complications should not affect the osteoblasts and trouble tissue homeostasis and healing. The obtained *in vitro* data confirm the cytotoxicity of chlorhexidine directly applied onto osteoblasts when used at concentrations exceeding 1 μM (approximately 0.00006 %). The direct application of chlorhexidine at higher concentrations during regenerative therapy for the treatment of peri-implantitis could thus have serious toxic effects on alveolar osteoblasts. However, the use of chlorhexidine mouthwashes (0.12 %) after implant installation is almost routine practice to maintain peri-implant health. Obviously, the contact is only for a few seconds or minutes *via* mucous membrane in this case. Interestingly, patients irrigating with diluted chlorhexidine (0.06 %, which is still far above the concentrations released in our setup) using a powered oral irrigator with a special subgingival irrigating tip showed reduced infection symptoms compared to patients rinsing with 0.12 % chlorhexidine gluconate once daily and is recommended as a valuable adjunct to oral health in patients with dental implants (Felo *et al.*, 1997). These results suggest that tackling the zone most proximal to the implant results in superior health outcome. This is precisely what is aimed for with the dental implant presented in this study, as it is capable of releasing chlorhexidine directly at the implant surface. Moreover, the observed chlorhexidine release concentrations of 0.005 % were sufficient to prevent *S. mutans* biofilm growth on the implant surface, suggesting that very low doses of an antibacterial compound are adequate when administered locally during a limited time. Due to the complex setup of the experiments it was not feasible to repeat the experiments using a lower range of chlorhexidine to determine the critical release concentration. However, recalling the reported MIC/BIC values of 1-3 μM, we estimate that a few μM would suffice, which is comparable to the reported cytotoxicity limit. Hence, in follow-up experiments, less cytotoxic compounds should additionally be evaluated for compatibility with our dental implant release system, for which chlorhexidine can serve as benchmark.

Indeed, our design allows for the insertion of other antibacterial compounds in the internal reservoir instead of chlorhexidine, such as antibiotics, thereby installing a very local antibiotics regimen for a prolonged time at the place of potential infections. Such local antibiotic dosing regimen, avoiding their systemic use, can be very attractive as the latter is associated with antibiotic resistance development. Moreover, the design of the Ti/SiO$_2$ composite dental implant presented in this manuscript enables a personalised treatment. Different antimicrobial compounds or antibiotics can be applied in the internal reservoir depending on the patient's need. Moreover, it is hypothesised that consecutive release of different

antimicrobial compounds or higher doses of the initial compound is possible by refilling the reservoir. This might be of interest in cases where the applied drug/dose appears to be ineffective. Additionally, simultaneous release of multiple compounds is envisaged as well, since combination therapy offers several advantages compared to single compound treatment of both bacterial and fungal biofilm infections (Blackledge *et al.*, 2013; De Cremer *et al.*, 2015). Once clinical and radiographic data indicate successful implant osseointegration, there is obviously no need for continued prophylaxis (preventive setup). If signs of peri-implantitis would emerge on osseointegrated implants at a later stage, the treatment by reversible, controlled release and repeatable drug administration can be started and stopped at any time (curative setup).

In conclusion, we provide a proof of concept of the sustained release of an antimicrobial compound from an internal reservoir through the Ti/SiO$_2$ material to the implant outer surface and surroundings. Release of this antimicrobial compound prevents and eradicates microbial biofilm formation on the rough implant surface, decreasing the risk for development of peri-implant diseases. Responding to the current need for more personalised treatments, our flexible implant design allows for the use of a broad range of antimicrobial compounds (alone or in combination) and fine-tuning of the concentration at which these are released will depend on the patient's need. This study focuses on dental implant applications, but the concept could, in principle, be translated to any percutaneous implant that can incorporate an internal reservoir, such as percutaneous fixation devices, as long as this does not compromise the mechanical strength of such load-bearing devices.

References

Aerts CA, Verraedt E, Depla A, Follens L, Froyen L, Van Humbeeck J, Augustijns P, Van den Mooter G, Mellaerts R, Martens JA (2010) Potential of amorphous microporous silica for ibuprofen controlled release. Int J Pharm **397**: 84-91.

Belibasakis GN, Charalampakis G, Bostanci N, Stadlinger B (2015) Peri-implant infections of oral biofilm etiology. Adv Exp Med Biol **830**: 69-84.

Bencharit S, Byrd WC, Altarawneh S, Hosseini B, Leong A, Reside G, Morelli T, Offenbacher S (2014) Development and applications of porous tantalum trabecular metal-enhanced titanium dental implants. Clin Implant Dent Relat Res **16**: 817-826.

Bhaskara Rao B V, Mukherji R, Shitre G, Alam F, Prabhune AA, Kale SN (2014) Controlled release of antimicrobial Cephalexin drug from silica microparticles. Mater Sci Eng C Mater Biol Appl **34**: 9-14.

Bhattacharyya S, Agrawal A, Knabe C, Ducheyne P (2014) Sol-gel silica controlled release thin films for the inhibition of methicillin-resistant *Staphylococcus aureus*. Biomaterials **35**: 509-517.

Blackledge MS, Worthington RJ, Melander C (2013) Biologically inspired strategies for combating bacterial biofilms. Curr Opin Pharmacol **13**: 699-706.

Braem A, Van Mellaert L, Mattheys T, Hofmans D, De Waelheyns E, Geris L, Anné J, Schrooten J, Vleugels J (2014) Staphylococcal biofilm growth on smooth and porous titanium coatings for biomedical applications. J Biomed Mater Res A 1**02**: 215-224.

Braem A, De Cremer K, Delattin N, De Brucker K, Neirinck B, Vandamme K, Martens JA, Michiels J, Vleugels J, Cammue BPA, Thevissen K (2015) Novel anti-infective implant substrates: controlled release of antibiofilm compounds from mesoporous silica-containing macroporous titanium. Colloids Surf B Biointerfaces **126**: 481-488.

Busscher HJ, Rinastiti M, Siswomihardjo W, van der Mei HC (2010) Biofilm formation on dental restorative and implant materials. J Dent Res **89**: 657-665.

Campoccia D, Montanaro L, Arciola CR (2013) A review of the biomaterials technologies for infection-resistant surfaces. Biomaterials **34**: 8533-8554.

Clark PA, Moioli EK, Sumner DR, Mao JJ (2008) Porous implants as drug delivery vehicles to augment host tissue integration. FASEB J **22**: 1684-1693.

Clarke JK (1924) On the bacterial factor in the aetiology of dental caries. Br J Exp Pathol **5**: 141-147.

Cline NV, Layman DL (1992) The effects of chlorhexidine on the attachment and growth of cultured human periodontal cells. J Periodontol **63**: 598-602.

Dalwai F, Spratt DA, Pratten J (2006) Modeling shifts in microbial populations associated with health or disease. Appl Environ Microbiol **72**: 3678-3684.

De Cremer K, Staes I, Delattin N, Cammue BP, Thevissen K, De Brucker K (2015) Combinatorial drug approaches to tackle *Candida albicans* biofilms. Expert Rev Anti Infect Ther **13**: 973-984.

de Freitas MM, da Silva CHP, Groisman M, Vidigal GM (2011) Comparative analysis of microorganism species succession on three implant surfaces with different roughness: an *in vivo* study. Implant Dent **20**: e14-23.

do Prado RF, de Vasconcellos LGO, de Vasconcellos LMR, Cairo CAA, Leite Dde O, dos Santos A, Jorge AO, Romeiro Rde L, Balducci I, Carvalho YR (2013) *In vivo* osteogenesis and *in vitro* Streptococcus mutans adherence: porous-surfaced cylindrical implants *vs.* rough-surfaced threaded implants. Int J Oral Maxillofac Implants **28**: 1630-1638.

Donelli G, Vuotto C (2014) Biofilm-based infections in long-term care facilities. Future Microbiol **9**: 175-188.

Esposito M, Coulthard P, Thomsen P, Worthington H V (2005) Interventions for replacing missing teeth: different types of dental implants. Cochrane database Syst Rev: CD003815.

Felo A, Shibly O, Ciancio SG, Lauciello FR, Ho A (1997) Effects of subgingival chlorhexidine irrigation on peri-implant maintenance. Am J Dent **10**: 107-110.

Giannelli M, Chellini F, Margheri M, Tonelli P, Tani A (2008) Effect of chlorhexidine digluconate on different cell types: a molecular and ultrastructural investigation. Toxicol In Vitro **22**: 308-317.

Gimeno M, Pinczowski P, Pérez M, Giorello A, Martínez MÁ, Santamaría J, Arruebo M, Luján L (2015) A controlled antibiotic release system to prevent orthopedic-implant associated infections: An *in vitro* study. Eur J Pharm Biopharm **96**: 264-271.

Goodman SB, Yao Z, Keeney M, Yang F (2013) The future of biologic coatings for orthopaedic implants. Biomaterials **34**: 3174-3183.

Goodson JM (2003) Gingival crevice fluid flow. Periodontol 2000 **3**1: 43-54.

Hasan J, Crawford RJ, Ivanova EP (2013) Antibacterial surfaces: the quest for a new generation of biomaterials. Trends Biotechnol **3**1: 295-304.

Hickok NJ, Shapiro IM (2012) Immobilized antibiotics to prevent orthopaedic implant infections. Adv Drug Deliv Rev **64**: 1165-1176.

Junka AF, Szymczyk P, Smutnicka D, Kos M, Smolina I, Bartoszewicz M, Chlebus E, Turniak M, Sedghizadeh PP (2015) Microbial biofilms are able to destroy hydroxyapatite in the absence of host immunity *in vitro*. J Oral Maxillofac Surg **73**: 451-64.

Lyndon JA, Boyd BJ, Birbilis N (2014) Metallic implant drug/device combinations for controlled drug release in orthopaedic applications. J Control Release **179**: 63-75.

Marcantonio C, Nicoli LG, Junior EM, Zandim-Barcelos DL (2015) Prevalence and Possible Risk Factors of Peri-implantitis: A Concept Review. J Contemp Dent Pract **16**: 750-7.

Mariotti AJ, Rumpf DA (1999) chlorhexidine-induced changes to human gingival fibroblast collagen and non-collagen protein production. J Periodontol **70**: 1443-1448.

Nicu EA, Van Assche N, Coucke W, Teughels W, Quirynen M (2012) RCT comparing implants with turned and anodically oxidized surfaces: a pilot study, a 3-year follow-up. J Clin Periodontol **39**: 1183-1190.

Park YS, Cho JY, Lee SJ, Hwang CI (2014) Modified titanium implant as a gateway to the human body: the implant mediated drug delivery system. Biomed Res Int 2014: 801358.

Pedrazzi V, Escobar EC, Cortelli JR, Haas AN, Andrade AK, Pannuti CM, Almeida ER, Costa FO, Cortelli SC, Rode Sde M (2014) Antimicrobial mouthrinse use as an adjunct method in peri-implant biofilm control. Braz Oral Res **28**.

Perez LM, Lalueza P, Monzon M, Puertolas JA, Arruebo M, Santamaría J (2011) Hollow porous implants filled with mesoporous silica particles as a two-stage antibiotic-eluting device. Int J Pharm **409**: 1-8.

Pucher JJ, Daniel JC (1992) The effects of chlorhexidine digluconate on human fibroblasts *in vitro*. J Periodontol **63**: 526-532.

Ribeiro M, Monteiro FJ, Ferraz MP (2012) Infection of orthopedic implants with emphasis on bacterial adhesion process and techniques used in studying bacterial-material interactions. Biomatter **2**: 176-194.

Santamaría E, Maestro A, Porras M, Gutiérrez JM, González C (2014) Controlled release of ibuprofen by meso-macroporous silica. J Solid State Chem **210**: 242-250.

Santos A, Sinn Aw M, Bariana M, Kumeria T, Wang Y, Losic D (2014) Drug-releasing implants: current progress, challenges and perspectives. J Mater Chem B **2**: 6157.

Shibli JA, Martins MC, Ribeiro FS, Garcia VG, Nociti FH, Marcantonio E (2006) Lethal photosensitization and guided bone regeneration in treatment of peri-implantitis: an experimental study in dogs. Clin Oral Implants Res **17**: 273-281.

Subramani K, Jung RE, Molenberg A, Hammerle CHF (2009) Biofilm on dental implants: a review of the literature. Int J Oral Maxillofac Implants **24**: 616-626.

Taniguchi Y, Kakura K, Yamamoto K, Kido H, Yamazaki J (2015) Accelerated osteogenic differentiation and bone formation on zirconia with surface grooves created with fiber laser irradiation. Clin Implant Dent Relat Res **18**: 883-894.

Varoni E, Tarce M, Lodi G, Carrassi A (2012) chlorhexidine (CHX) in dentistry: state of the art. Minerva Stomatol **61**: 399-419.

Verraedt E, Pendela M, Adams E, Hoogmartens J, Martens JA (2010) Controlled release of chlorhexidine from amorphous microporous silica. J Control Release **142**: 47-52.

Yuan K, Chan YJ, Kung KC, Lee TM (2014) Comparison of osseointegration on various implant surfaces after bacterial contamination and cleaning: a rabbit study. Int J Oral Maxillofac Implants **29**: 32-40.

Discussion with Reviewer

Llinos Harris: How effective is the system on the other bacteria that are commonly present in the mouth? Is it possible that the eradication of *S. mutans* could lead to other species flourishing and causing infections?

Authors: Chlorhexidine is known to be a broad-spectrum biocide effective against Gram-positive bacteria, Gram-negative bacteria and fungi. To show the effectiveness of our system, we have performed additional experiments and demonstrated biofilm-preventing activity of chlorhexidine released through Ti/SiO₂ disks against *Candida albicans* biofilms, a yeast species known to be involved in dental infections (Fig. 8).
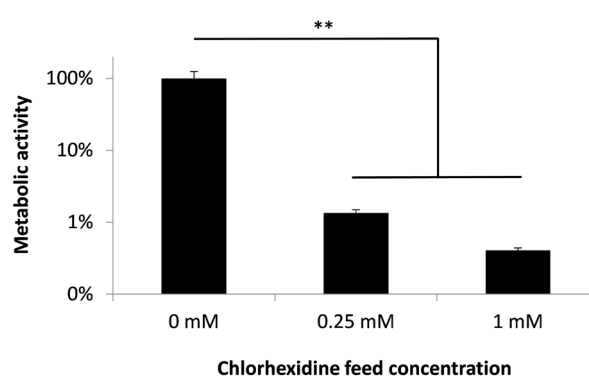

Fig. 8. Prevention of *C. albicans* biofilm formation on chlorhexidine-releasing Ti/SiO₂ disks. Different concentrations of chlorhexidine were applied to the feed reservoir in the *in vitro* test tool. Values are mean metabolic activity of 72 h old *C. albicans* biofilms ± standard error ($n = 3$), measured by CTB staining. The asterisks indicate a statistically significant difference in metabolic activity (** $p < 0.01$).

Llinos Harris: Do the authors know what would happen to the osteoblasts if exposed to the initial burst release observed in the first 3 d?

Authors: We have assessed release kinetics of chlorhexidine (Fig. 3**a**) and we described a steady release of chlorhexidine from day 3 without initial burst (resulting in mean chlorhexidine release of 9 nmol/cm²) for the lowest feed concentration (0.1 µM chlorhexidine). In our set-up, this corresponds to 33 µM chlorhexidine – a dose with *in vitro* toxicity to osteoblasts. However, it should be noted that compounds administered into the periodontal pocket are rapidly washed out *in vivo* (Goodson, 2003). Therefore we anticipate that *in vivo* chlorhexidine release is gradually cleared by the surrounding tissue, resulting in lower net chlorhexidine concentrations. Hence, it is very difficult to predict *in vivo* toxicity associated with chlorhexidine release from our device based on the current *in vitro* data. As a consequence, the data from this study have to be seen in a broader context, namely as a proof of concept, which can be extended to the use of any bioactive, potentially less toxic, compound.

Britt Wildermann: Can you make any assumption regarding the effect of cells growing on the implant and the release kinetics. Due to the fact that the implant should be integrated, the pores might be filled/covered by cells. Would this then stop the release and hinder the envisioned use to cure a late infection?

Authors: At present, we have no data on the effect of osteoblast growth on the material and potential clogging of the mesopores, thereby hindering release of the antimicrobial compound. *In vivo* follow-up studies are necessary to provide data in this regard. Nevertheless, in a preventive set-up, no cells are present immediately after implant installation when infections are most common to occur. When compounds should be administered for

curative reasons, the infection is often associated with bone loss which will (re-)enable release of compounds.

Britt Wildermann: Information regarding the mechanical properties would be interesting. Do these implants fulfil the requirements of dental implants?

Authors: This important issue will need to be explored in order to take the current proof of concept further to a potential clinical implementation. The presence of micropores in the titanium implant will inherently reduce its mechanical strength, while fatigue cracks can initiate at the open surface pores reducing its endurance limit. However, it is not well understood how the presence of a second phase (SiO$_2$) inside the micropores will influence the mechanical behaviour of the composite material. Therefore, future work will focus on the characterisation of the mechanical properties of the designed implants.

Reto Luginbuehl: Do you have data on blocking of the pores by adsorbed proteins or calcification?

Authors: The pores of the silica correspond to the void volumes generated by crosslinking of spherical nanoparticles. The 3D porous network facilitates molecular transport and minimises the risk of pore blockage, especially for relatively smaller molecules like chlorhexidine. Currently, there is no data available on how the adsorption of macromolecules/proteins (from the implant environment) or bone formation on the implants outer surface will influence the controlled release of the bioactive target molecules (such as the chlorhexidine used in this study). The controlled release is a diffusion process driven by a concentration difference of the target molecule between the internal reservoir and the implant surroundings. We anticipate that the presence of proteins or bone on the implant surface will slow down the dissipation of the target molecule and lead to a local build-up. As such, the driving force for the diffusion through the implant will be less. However, when infections occur, this is usually accompanied by bone loss, so that the concentration of the target molecule at the implant surface will drop again, in turn increasing the release from the implant.

T. Fintan Moriarty: Does the internal cavity/reservoir refill with physiological fluids after antimicrobials have released? Presumably, the release of antibiotic will not result in a vacuum within the implant and if the reservoir can be refilled with fluid entering between the cover screw and implant, could the reservoir also become colonised by oral microflora?

Authors: Indeed, we hypothesise that release of the antimicrobial agent from the reservoir will not result in a vacuum, but will probably allow water molecules (which can migrate through the mesopores) to migrate to the cavity. However, this will not be possible for the microbial cells as these are too big (approx. 0.2-1 μm micro-organism size *versus* 6 nm pore size). As indicated in the Materials and Methods section, we used a stainless steel cover screw (M2 × 2.25) for flexible refilling of the internal reservoir. This cover screw is equipped with a conical surface mating the 2° countersink in the implant abutment in order to provide a sealing surface that effectively prevents leakage of the drug solution to the oral cavity and vice versa. Hence, we do not anticipate that fluid can enter the cavity through the cover screw.

Editor's note: The Scientific Editor responsible for this paper was T. Fintan Moriarty.